

## SPATIAL RESPONSE OF WAVY VORTEX FLOW TO AXIAL OSCILLATIONS OF THE INNER CYLINDER

Manish Sinha,<sup>1\*</sup> Ioannis G. Kevrekidis<sup>2</sup> and Alexander J. Smits<sup>1</sup>

<sup>1</sup>Gas Dynamics Laboratory, Forrestal Campus, Princeton University, Princeton, NJ, 08540, U.S.A.

<sup>2</sup>Chemical Engineering & PACM, Princeton University, Princeton, NJ, 08544, U.S.A.

\*Corresponding author: Manish Sinha, msinha@princeton.edu

### Abstract

We study the response of wavy vortex flow to time-periodic axisymmetric axial forcing. This is accomplished by examining the flow pattern in a variation of the classical Taylor-Couette system: in a long aspect ratio, narrow gap facility the outer cylinder is held stationary while the inner cylinder rotates at constant angular velocity and simultaneously executes harmonic oscillations in the axial direction. Using kalliroscope suspension, we have obtained experimental visualization of the flow pattern for various combinations of axial and rotational Reynolds numbers. The response of wavy vortex flow to imposed axial forcing is presented. In addition to obtaining snapshots of the flow around the entire apparatus through multiple cameras, the axial and azimuthal wave numbers are measured and plotted above the initial stability boundary. For constant rotation rates, increasing axial forcing leads to an initial drop in the axial wave number followed by a subsequent rise, while the azimuthal wave number appears to be unaffected. In addition, it reduces the amplitude of the waviness while destabilizing the flow by disrupting the spatial regularity of the vortex pattern. For constant forcing amplitudes, increasing rotation rates lead to increasing azimuthal wave numbers coupled by a simultaneous, eventual, rise in the axial wave number.

### Introduction

When time-periodic axial forcing is imposed on regular Taylor-Couette flow, it raises the rotation rate required for transition to Taylor vortex flow (TVF) and subsequent wavy vortex flow [1,2]. In effect, the boundary separating helical Couette flow (HCF) - the base flow state, consisting of circular Couette flow and annular Stokes flow - and some variation of TVF is a surface in  $(Re_{ax}, \bar{\omega}, Re_{\Omega})$  space. When this surface is cut by a vertical plane of the form  $Re_{ax} = c\bar{\omega}$ , where  $c$  is some constant, the 3D surface becomes a 2D curve. This curve may be obtained experimentally, or computationally through Floquet analysis of the basic HCF as in [2,3]. However, this analysis is valid only close to the primary bifurcation curve and the spatial structure in the nonlinear regime far above the boundary cannot be obtained from this method. The current experiment maps out the flow field characteristics in both the linear and nonlinear regime. This curve, shown in Fig. 1, is large enough so that it encompasses transitions to both periodic and quasi-periodic flows [3,4]. This allows one to examine if the flow structure in a given region is peculiar in any way, and if there is a correlation between the character of the spatial and particular temporal features.

Four dimensionless parameters define the problem though only three define the critical surface, since two of them (eqns. (1) and (3)) are related in our apparatus. However, only equations (1) and (2) are strictly independent variables. The four parameters

are: (i)  $Re_{ax}$  (axial Reynolds number), (ii)  $Re_{\Omega}$  (azimuthal Reynolds number), (iii)  $\bar{\omega}$  (non-dimensional axial forcing frequency) and (iv)  $f_{app}$  (applied frequency ratio). They are defined as follows:

$$Re_{ax} = Ud / \nu \quad (1)$$

$$Re_{\Omega} = \Omega r_i d / \nu \quad (2)$$

$$\bar{\omega} = \omega_j d^2 / \nu \quad (3)$$

$$f_{app} = \omega_j / \Omega \quad (4)$$

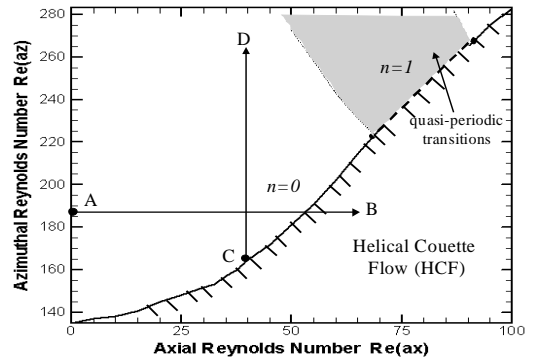


Figure 1: Primary critical surface separating the basic HCF state (*below*) from flow regimes containing Taylor cells (*above*); constructed from [2,3].

The objective is to map out the region above the primary stability boundary in axial ( $n$ ) and azimuthal ( $k$ ) wave number space, i.e. ( $n,k$ ) space for every point above the curve. Furthermore, the actual flow pattern needs to be obtained around the entire apparatus in order to unambiguously characterize the flow state. Once the various flow states above the critical surface have been mapped out, one is able to discuss the following two problems: (a) the response of wavy vortex flow to increasing axial forcing (path AB), and (b) the response of some flow state just above the critical surface (i.e. some tilted  $n=0$  mode) to increasing rotation rates (path CD).

## Methods

The apparatus described in [1,4] was used in this study. The inner and outer cylinder diameters were  $d_i = 0.0763$  m and  $d_o = 0.0843$  m respectively. The aspect ratio,  $L/d$ , was 152 and the radius ratio,  $\eta$ , was 0.905. Axial and rotational motions of the inner cylinder were controlled separately. Due to the Scotch yoke mechanism coupling  $U$  and  $\omega_f$ , the axial Reynolds number and non-dimensional forcing frequency are linearly related. A schematic of the experimental arrangement is shown in Fig. 2.

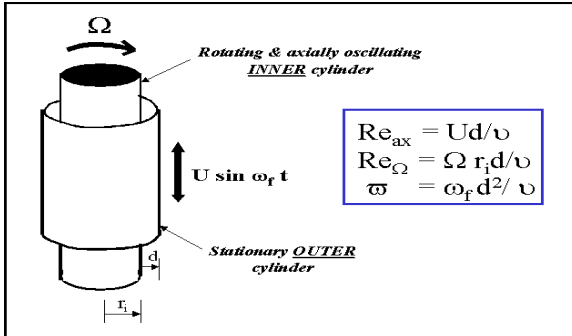


Figure 2: Apparatus schematic depicting cylinder motion.

Four Polaroid digital cameras were placed 90 degrees apart around the apparatus at a fixed height. Images from each were acquired simultaneously and later used to reconstruct flow snapshots around the entire apparatus. Due to the surrounding oil bath, refraction effects were eliminated.

A separate CCD camera was used for the axial wave number measurements. These were calculated in two different ways. The gray scale variation down a vertical slice within the center of the image was plotted and the axial wavelength was readily deduced from the intersection of this curve with a line of constant gray scale value. In addition, the vertical

gray scale distribution was passed through a Fast Fourier Transform algorithm. The position of the dominant peak was directly related to the axial wavelength.

Measurement of the azimuthal wave number was straightforward - one merely counts the number of waves in the surround view. The axial wave number measurement, however, is subject to the following potential sources of error. When  $Re_{ax}$  is large, isolated inhomogeneities may occur which lead to a slight disruption to the axial periodicity. When this occurs one must wait for a snapshot that does not contain such inhomogeneities as they can lead to errors in the axial wavelength measurement. Near the critical surface the vortices are not strong and only a portion of the axial window may contain vortices. In this case the vertical extent and corresponding FFT window must be correspondingly adjusted. Finally, three flow snapshots at random times are acquired at the given Reynolds numbers and used to obtain an average axial wave number. It is assumed, naturally, that  $k$  therefore does not vary with time at a given flow setting. Although the dynamic competition between the forcing and rotation will lead to a time-varying axial fluid transfer between vortices, it is assumed that this does not affect the wavelength; merely the vortex growth rate and cell diameter of the vortices.

The working fluid used throughout was a 20:1 suspension of water and Kalliroscope AQ-1000 rheoscopic concentrate. The Kalliroscope flakes align themselves with the local shear stress thereby making flow patterns visible. Initially, azimuthal motion only was imparted to the inner cylinder. The azimuthal Reynolds number acceleration rate,  $dRe_{\Omega}/dt$ , was  $0.3s^{-1}$ . After the desired azimuthal Reynolds number was reached, the flow was allowed to settle for about 30 viscous time scales,  $t_v$ , defined below.

$$t_v = d^2/\nu \quad (5)$$

At this point, axial motion was initiated. Once again  $dRe_{ax}/dt$  was  $0.3s^{-1}$  and the flow was allowed to settle for 30 viscous time scales before acquiring images. One-parameter cuts with increasing axial Reynolds number were performed. Snapshots at constant  $Re_{\Omega}$  with steps in  $Re_{ax}$  of 10 were then acquired.

Unlike in [4] the temperature was not controlled through an electronic feedback system. Instead at each constant  $Re_{\Omega}$  cut the temperature was continually monitored. The maximum temperature fluctuation measured was  $\pm 0.15^{\circ}C$ .

## Results

The experimentally determined axial wave number at the transition from circular Couette flow to Taylor vortex flow is in excellent agreement with that predicted from analytical techniques. The measured value is  $3.12 \pm 0.06$ , in good accordance with that obtained from Floquet analysis [2] of 3.129. For constant rotation rates, the effect of axial forcing on the measured axial wave number is shown in Fig. 3.

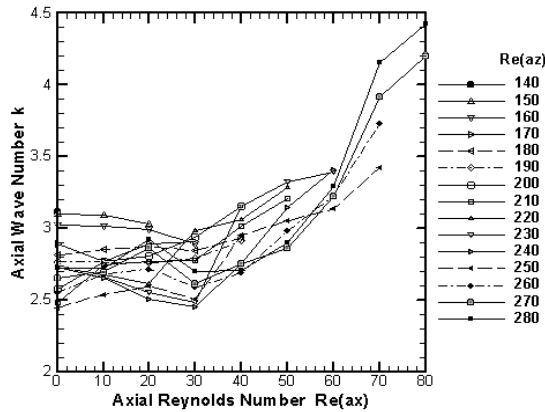


Figure 3: Effect of axial forcing on axial wave number for constant azimuthal Reynolds number.

For small amplitudes of forcing, generally  $Re_{ax}$  up to about 40, the axial wave number changes little; small decreases are observed balanced by small increases. However, for  $Re_{ax}$  above 40 the trend is markedly different. The axial wave numbers rise rapidly by about 45% from an  $Re_{ax}$  of 40 up to an  $Re_{ax}$  of 80. As the amplitude of the forcing rises then so does the amount of fluid transported axially between individual cells, and we have competition between Couette flow and Stokes flow. The wave number for the most unstable mode with purely Couette flow is about  $\pi$  while that for purely axial Stokes flow is 0. Thus, as the axial component increases one would expect the Stokes component to bring about a reduction in the axial wave number. This appears, fairly weakly, to occur for  $Re_{ax}$  up to about 40. Exactly why a further increase in the Stokes component should initiate a dramatic increase in the wave number is not obvious. It is possible that vortex pairs may be increasing in numbers when the forcing amplitude becomes very high, or that the forcing congregates more pairs in the centre of the facility than at the ends. Assuming just the former effect were at play, a 50% increase in the number of vortex pairs would be needed to account for the observed increase in  $k$  from  $\sim 2.8$  to  $\sim 4.3$ .

For increasing rotation rates at fixed amplitudes of forcing, the wave number dependence is shown in Fig. 4.

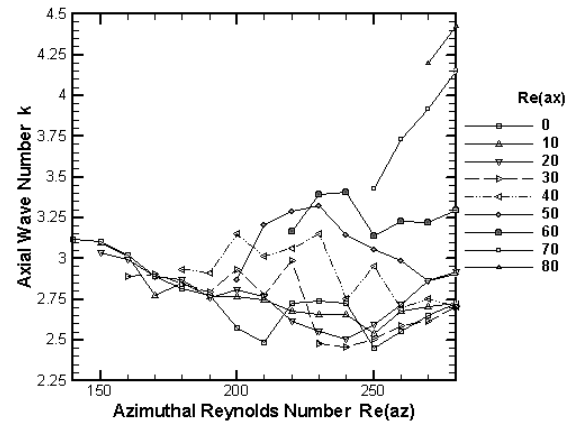


Figure 4: Effect of azimuthal rotation on axial wave number for constant axial Reynolds number.

For  $Re_{ax}$  up to about 30, there is a generally slow decrease in axial wave number up to about  $Re_{\Omega} \sim 200$ . Between 200 and 250 the axial wave number varies unpredictably while above 250 it generally rises monotonically. For  $Re_{ax}$  equal to 50 and 60, an initial rapid increase is observed followed by a gradual reduction to about the initial value of  $k$ . However for  $Re_{ax}$  of 70 and 80 we observe only a steep rise in  $k$ .

The effect of increasing rotation rates on the azimuthal wave number is shown in Fig 5.

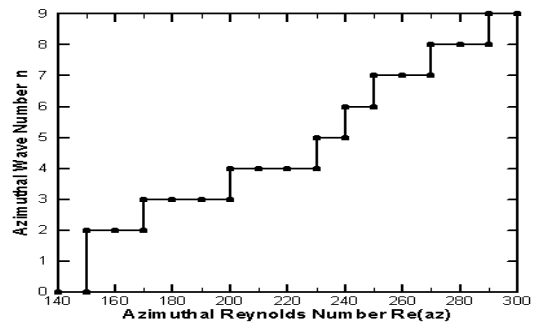


Figure 5: Effect of azimuthal Reynolds number on the azimuthal wave number.

The  $n=1$  azimuthal mode is not observed. No single mode persists for a large interval in Reynolds number. Some azimuthal modes appear and disappear with the minimum change in  $Re_{\Omega}$  considered. Due to the imposed step size in  $Re_{\Omega}$ , the boundaries between distinct azimuthal modes are known only within an

error of  $Re_\Omega$  of 10. Observations indicate that once a given wavy mode has been established, axial forcing does not affect the azimuthal wave number. Rather, the amplitude of the waviness is reduced until it is virtually undetectable close to the transition surface, say within an axial Reynolds number of 10 from the critical value. According to [3] axial oscillations of the inner cylinder destabilize non-axisymmetric wavy modes. In our observations such forcing leads to the gradual emergence of inhomogeneities which reduce the periodicity in the flow pattern. Occasional vortex “mis-matching”, appearing qualitatively similar to vortex dislocations, become more common as the forcing amplitude is raised.

Surround views may be seen in Fig. 6. All are for

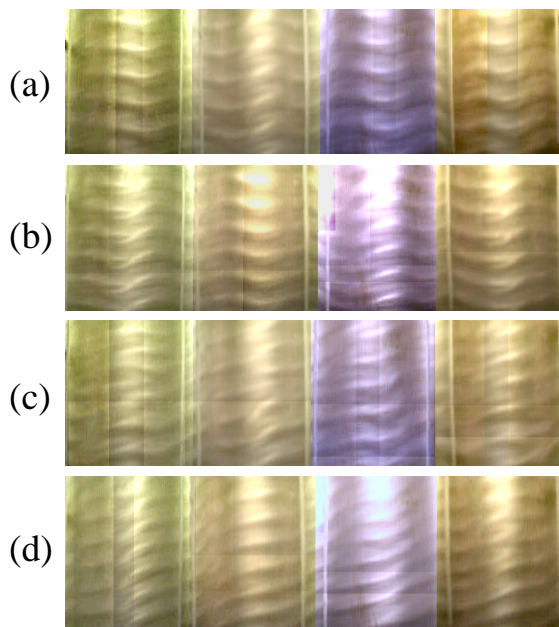


Figure 6: Surround images showing the effect of increasing axial forcing on wavy vortex flow

$Re_\Omega$  of 240 but for increasing forcing amplitude: images (a), (b), (c) and (d) are for  $Re_{ax}$  of 0, 20, 40 and 60 respectively. It is clear that the interaction of the axisymmetric forcing with the non-axisymmetric wavy vortex flow generates a non-axisymmetric flow state. The cells are now not closed but form a spiral pattern. The maximum inclination of this ring increases with forcing amplitude. Image (d) contains a higher axial wave number than (a), consistent with Fig. 3. Even for small forcing amplitudes, say  $Re_{ax}$  equal to 20, the vortex structure appears to be inclined. As the forcing amplitude rises, the amplitude of the cell waviness reduces while the azimuthal wave number appears to be unaffected.

## Conclusions

The response of a time-varying, *non-axisymmetric* flow to time-periodic, axisymmetric disturbances has been investigated. This was achieved by studying the effect of harmonic axial oscillations of the inner cylinder on wavy vortex flow in a Taylor-Couette apparatus. Recent computations have investigated the effect of time-varying, axisymmetric disturbances to a time-periodic, *axisymmetric* flow [2], namely helical Couette flow. Thus, the complexity of our *unforced* system has increased by losing axisymmetry.

For constant rotation rates, the axial forcing generally leads to an increase in the axial wave number, particularly for larger forcing amplitudes. However, the azimuthal wave number was virtually unaffected while the amplitude of the waviness was increasingly suppressed. For constant forcing amplitudes, azimuthal rotation initiated higher order instabilities, manifest through increasing azimuthal wave numbers. Increasing rotation rates also eventually lead to an increase in axial wave number.

Surround views of the flow were also obtained for various flow states. The images provided direct, unambiguous determination of the azimuthal wave number. In the presence of axial forcing the surround images revealed a break in the closed loop cells found in wavy vortex flow, and illustrated the breakdown of that flow state through a loss of structural periodicity.

## Acknowledgements

Kind permission from F. Marques and J.M. Lopez to produce Fig. 1 from [2,3] are much appreciated. The work was supported through NSF Grant CTS97-06902

## References

- [1] Weisberg, A.Y., Kevrekidis, I.G. and Smits, A.J., 1997, "Delaying transition in Taylor-Couette flow with axial motion of the inner cylinder," *J. Fluid Mech.*, 348:141-151.
- [2] Marques, F. and Lopez, J.M., 1997, "Taylor-Couette flow with axial oscillations of the inner cylinder: Floquet analysis of the basic flow," *J. Fluid Mech.*, 348:153-175.
- [3] Marques, F. and Lopez, J.M., 2000, "Spatial and temporal resonances in a periodically forced hydrodynamic system," *Physica D*, 136:340-352.
- [4] Sinha, M., Kevrekidis, I.G., and Smits, A.J., 2001, "Dynamics and quasi-periodicity in axially forced Taylor-Couette flow," 5<sup>th</sup> World Congress on Experimental Heat Transfer, Fluid Mechanics and Thermodynamics, Thessaloniki, Greece, 24-28 Sept., *to be published*.